

Optimizing Sampling Rate of P&O MPPT Technique

N.Femia, G.Petrone, G.Spagnuolo
D.I.I.E. – University of Salerno, Italy
I-84084, Fisciano (SA) – ITALY
Email: femia@unisa.it, gpetrone@unisa.it,
spanish@ieee.org

M.Vitelli
D.I.I. – Second University of Naples, Italy
Real Casa dell'Annunziata, Aversa (CE), Italy
Email: vitelli@unina.it

Abstract—This paper shows that the efficiency of the Perturb and Observe (P&O) Maximum Power Point Tracking (MPPT) control technique can be improved by optimizing its sampling interval T_s according to the converter's dynamics. During sunny days, when the maximum power point of the photovoltaic (PV) array moves very slowly, the sampling interval T_s must be set as short as possible without causing instability. If the algorithm samples the array voltage and current too quickly, it is subjected to possible mistakes caused by the transient behavior of the PV array+converter system, thus missing temporarily the MPP. As a consequence, the algorithm can be confused, the energy efficiency decays, and the operating point can become unstable, entering disordered behaviors. The solution proposed in this paper lies in choosing T_s according to the converter's dynamics. The choice of the value of T_s according to the proposed approach ensures a three-level steady-state duty-cycle swing around the MPP, whatever the duty-cycle step-size and the irradiance level are. As an example, a boost MPPT battery charger has been studied.

I. INTRODUCTION

A photovoltaic (PV) array under uniform irradiance exhibits a current-voltage characteristic with a unique maximum power point (MPP) where the array produces maximum output power, which changes as a consequence of the variation of the irradiance level and of the panels' temperature [1]. The issue of maximum power point tracking (MPPT) has been addressed in different ways in the literature [2-10]: fuzzy logic, neural networks, pilot cells and DSP based implementations have been proposed. But, especially for low-cost implementations, the Perturb and Observe (P&O) and INcremental Conductance (INC) [2] techniques are widely used. In a typical P&O MPPT algorithm, the operating voltage of the PV array is perturbed by changing the duty-cycle in a given direction (increase or decrease) and the power drawn from the PV array is probed: if it increases, then the operating voltage is further perturbed in the same direction, whereas, if it decreases, then the direction of operating voltage perturbation is reversed. A drawback of P&O is that the operating point oscillates around the MPP, even during sunny days when the irradiance is slowly varying, giving rise to the waste of some amount of available energy. Several improvements of the P&O algorithm have been proposed in order to reduce the amplitude of oscillations around the MPP in steady state, at the price of slowing down the speed of response of the algorithm to changing atmospheric conditions and lowering the algorithm efficiency during cloudy days. The INC

algorithm seeks to overcome such limitations. However, as discussed in [12], because of noise and measurement and quantization errors, also the INC operating voltage oscillates around the MPP. Both methods can be confused during those time intervals characterized by changing atmospheric conditions, since the operating point can move away from the MPP instead of close to it [2]. In [12] it is shown that the P&O method, when properly optimized, leads to an efficiency which is equal to that obtainable by the INC method; however, no guidelines or general rules are provided therein allowing the identification of the optimal values of P&O parameters which are instead chosen through trial and error tests. This paper shows that the efficiency of P&O MPPT control technique can be improved by optimizing its sampling rate according to the converter's dynamics. As an example, a boost MPPT converter (fig.1) has been studied.

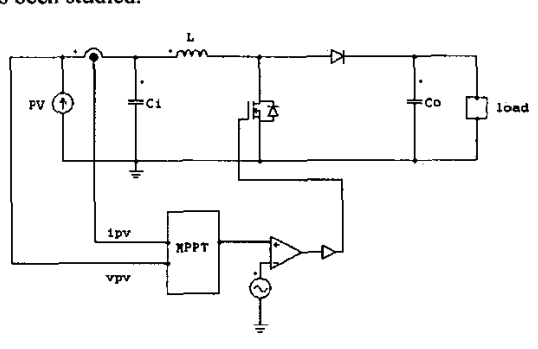


Fig. 1. A boost MPPT converter schematic.

Let T_s and Δd (>0) be respectively the sampling interval and the magnitude of the duty-cycle perturbation of the P&O MPPT algorithm. The duty cycle perturbation at the $(k+1)$ -th sampling is given by:

$$\begin{aligned} d((k+1)T_s) &= d(kT_s) \pm \Delta d = \\ &= d(kT_s) + (d(kT_s) - d((k-1)T_s)) \cdot \text{sign}(p((k+1)T_s) - p(kT_s)) \end{aligned} \quad (1)$$

Δd must be properly chosen: lowering Δd reduces the steady-state losses caused by the oscillation of the array operating point around the MPP but makes the algorithm less efficient in case of rapidly changing atmospheric conditions. The optimal choice of Δd in situations where we have to account for both the source's and converter's dynamics, is discussed in detail in the paper [13]. The case of quickly varying MPP occurs in cloudy days only. There is a more general problem, which occurs even during sunny

days where the MPP moves very slowly, connected to the choice of the sampling interval T_a of the P&O MPPT algorithm. Indeed, T_a must be set as short as possible without causing instability. In fact, considering a slowly-varying MPP, if the algorithm samples the array voltage and current too quickly, it is subjected to possible mistakes caused by the transient behavior of the PV array+converter system, thus missing temporarily the MPP. As a consequence, the algorithm can be confused, the energy efficiency decays, and the operating point can become unstable, entering disordered behaviors [12]. The solution proposed in this paper lies in choosing T_a according to the converter's dynamics, so that after each duty-cycle perturbation the system is allowed reaching steady-state operation before the next duty-cycle step variation.

II. THE MODEL

At MPP the adapted load resistance R is equal to the absolute value R_{MPP} of the differential resistance of the PV array. If the operating point of the PV array is close to the MPP, the power drawn by the PV array can be expressed as:

$$p(t) \cong \frac{v_{PV}^2(t)}{R_{MPP}} \quad (2)$$

The relation between the PV array terminal current and voltage is:

$$i_{PV} = I_H - I_s \cdot \left(e^{\frac{v_{PV} + R_s \cdot i_{PV}}{\eta \cdot V_T}} - 1 \right) - \frac{v_{PV} + R_s \cdot i_{PV}}{R_h} \quad (3)$$

where R_s and R_h are series and shunt resistances respectively, I_H is the light induced current, η is the diode ideality factor, I_s is the diode saturation current and V_T is the thermal voltage [1]. I_H depends on the irradiance level S and on the array temperature T , while I_s and V_T depend on T only [1]. Let the system be perturbed by a small duty-cycle step. If the oscillations of the operating point are small compared to the MPP then we get:

$$\hat{i}_{PV} = \left. \frac{\partial i_{PV}}{\partial v_{PV}} \right|_{MPP} \cdot \hat{v}_{PV} + \left. \frac{\partial i_{PV}}{\partial S} \right|_{MPP} \cdot \hat{S} + \left. \frac{\partial i_{PV}}{\partial T} \right|_{MPP} \cdot \hat{T} \quad (4)$$

Symbols with hats in the linearized equation (4) represent small-signal variations around the steady state values of the corresponding quantities. At constant (or slowly-varying) irradiance level, it is $\hat{S} = 0$. Moreover, at steady-state, due to the relatively high thermal inertia of the PV array [1], it is $\hat{T} \approx 0$. Eq. (4) can therefore be rewritten as:

$$\hat{i}_{PV} = \left. \frac{\partial i_{PV}}{\partial v_{PV}} \right|_{MPP} \cdot \hat{v}_{PV} \quad (5)$$

From eq. (3) we obtain:

$$\left. \frac{\partial i_{PV}}{\partial v_{PV}} \right|_{MPP} = - \left[R_s + \frac{\eta \cdot V_T \cdot R_h}{I_s \cdot R_h \cdot e^{\frac{v_{PV} + R_s \cdot i_{PV}}{\eta \cdot V_T}} + \eta \cdot V_T} \right]_{MPP}^{-1}$$

so that:

$$\left. \frac{\partial i_{PV}}{\partial v_{PV}} \right|_{MPP} = - \left[R_s + \frac{\eta \cdot V_T \cdot R_h}{I_s \cdot R_h \cdot e^{\frac{v_{MPP} + R_s \cdot i_{MPP}}{\eta \cdot V_T}} + \eta \cdot V_T} \right]^{-1}$$

and, finally:

$$\left. \frac{\partial i_{PV}}{\partial v_{PV}} \right|_{MPP} = - \frac{1}{R_{MPP}} \quad (6)$$

where v_{MPP} and i_{MPP} are the PV array MPP voltage and current respectively. In the neighborhood of the MPP, assuming $v_{PV} = v_{MPP} + \hat{v}_{PV}$ and $i_{PV} = i_{MPP} + \hat{i}_{PV}$ we have:

$$p = P_{MPP} + \hat{p} = v_{MPP} \hat{i}_{MPP} + v_{MPP} \hat{i}_{PV} + \hat{v}_{PV} i_{MPP} + \hat{v}_{PV} \hat{i}_{PV} \quad (7)$$

From eqs. (5)-(7), and considering that $v_{MPP} = R_{MPP} i_{MPP}$ at MPP, we get:

$$\hat{p} = v_{MPP} \hat{i}_{PV} + \hat{v}_{PV} i_{MPP} + \hat{v}_{PV} \hat{i}_{PV}$$

so that:

$$\hat{p} = \hat{v}_{PV} \left(i_{MPP} - \frac{v_{MPP}}{R_{MPP}} \right) + \hat{v}_{PV} \hat{i}_{PV} = - \frac{\hat{v}_{PV}^2}{R_{MPP}} \quad (8)$$

Eq. (8) shows that the dynamics of \hat{v}_{PV}^2 and that of \hat{p} is the same. The small signal equivalent circuit of the system under study can be solved to find the small-signal control-to-array voltage transfer function $G_{v_{pd}}$ and the load-to-array voltage transfer function $G_{v_{load}}$, such that $\hat{v}_{PV} = G_{v_{pd}} \cdot \hat{d} + G_{v_{load}} \cdot \hat{i}_{load}$. The transfer function $G_{v_{load}}$ gives the fluctuations of the array voltage caused by load variations; such fluctuations can confuse the MPPT algorithm, which is not able to distinguish between array voltage oscillations caused by the load or caused by the

modulation of the duty. As the P&O algorithm directly acts on d , our attention focuses on $G_{v_p,d}$.

The case of a boost battery charger is considered, for which $G_{v_p,d}$ assumes the following expression:

$$G_{v_p,d}(s) = \frac{\mu \cdot \omega_n^2}{s^2 + 2 \cdot \xi \cdot \omega_n \cdot s + \omega_n^2} \quad (10)$$

where $\mu = -V_o$, $\omega_n = \frac{1}{\sqrt{L \cdot C_i}}$ and $\xi = \frac{1}{2 \cdot R_{MPP}} \cdot \sqrt{\frac{L}{C_i}}$.

The Bode diagrams of $G_{v_p,d}$ are shown in fig. 3.a, with: $L=600 \mu\text{H}$, $C_i=100 \mu\text{F}$, $V_o=350 \text{ V}$, $R_{MPP}=45 \Omega$ (at $S=1000 \text{ W/m}^2$), $R_{MPP}=120 \Omega$ (at $S=350 \text{ W/m}^2$), $\xi=0.0986$ (at $S=1000 \text{ W/m}^2$), $\xi=0.0816$ (at $S=350 \text{ W/m}^2$), $\omega_n = 4082 \text{ rad/s}$. The 14 m^2 PV array is made by a series of 14 panel. Given the transfer function (10), the response of \hat{v}_{PV} to a small duty-cycle step perturbation of amplitude Δd is:

$$\hat{v}_{PV} = \mu \Delta d \left(1 - \frac{e^{-\xi \omega_n t}}{\sqrt{1-\xi^2}} \sin(\omega_n t \sqrt{1-\xi^2} + \cos^{-1} \xi) \right) \quad (11)$$

From eqs. (8) and (11), the response of \hat{p} to the step duty cycle perturbation Δd can be approximated as in eq.(12):

$$\begin{aligned} \hat{p} &= -\frac{\hat{v}_{PV}^2}{R_{MPP}} \approx \\ &\approx -\frac{\mu^2 \Delta d^2}{R_{MPP}} \left(1 - \frac{2e^{-\xi \omega_n t}}{\sqrt{1-\xi^2}} \sin(\omega_n t \sqrt{1-\xi^2} + \cos^{-1} \xi) \right) \end{aligned} \quad (12)$$

Therefore, the time T_e after which \hat{p} will be confined in the region $[-(1+\epsilon)\mu^2 \Delta d^2 / R_{MPP}, -(1-\epsilon)\mu^2 \Delta d^2 / R_{MPP}]$, centered around the steady-state value $-\mu^2 \Delta d^2 / R_{MPP}$ [14], is given by:

$$T_e \cong -\frac{1}{\xi \cdot \omega_n} \cdot \ln(\epsilon) \quad (13)$$

III. SIMULATION RESULTS

The responses of \hat{p} and \hat{v}_{PV} to a small duty cycle step perturbation ($\Delta d=0.01$) are shown respectively in fig. 3b and 3c.

The detailed view of the PV array voltage and of the duty cycle for the P&O controlled boost battery charger of fig. 4 shows that, if $T_a > T_e$, a sufficiently low value of ϵ ensures that the P&O MPPT algorithm is not confused by the transient behavior of the system.

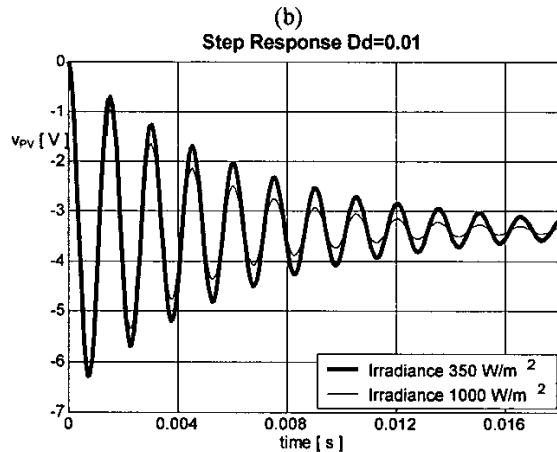
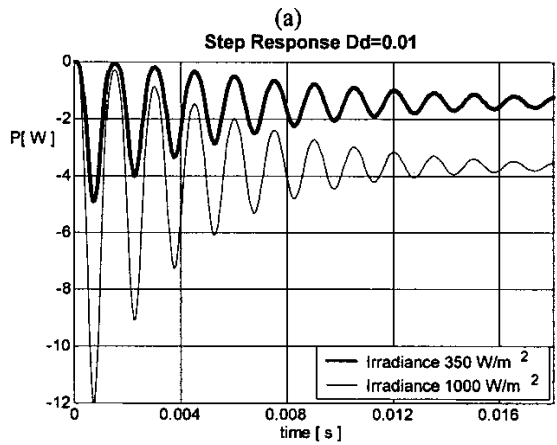
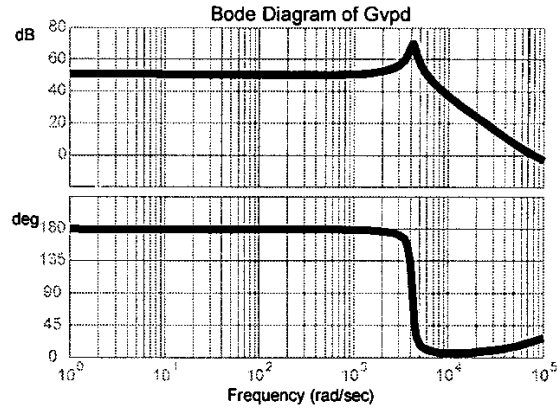


Fig. 3. Duty cycle step responses.

In this case, the duty-cycle assumes only three different values: $d_{MPP}-\Delta d$, d_{MPP} , $d_{MPP}+\Delta d$ (fig.5.a) and the operating point takes only three different positions on the PV array characteristic of fig.4.b: point C (on the right of the MPP), point B (close to the MPP) and point A (on the left of the MPP). It is worth noting that point B is not perfectly coincident with the MPP because of the discretization of d ;

of course, the lower Δd the lower either the distance between B and the MPP or the speed of response of the MPPT to changing atmospheric conditions.

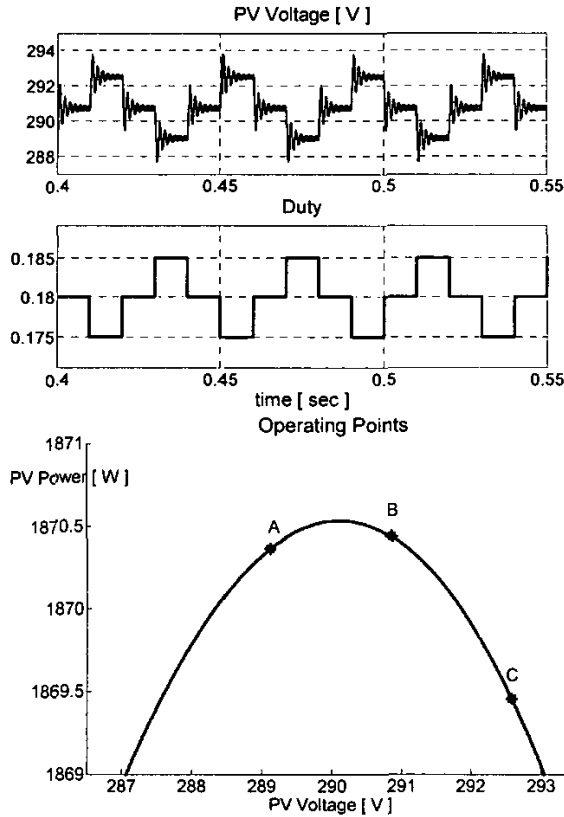


Fig. 4. $\epsilon=0.1, T_a=0.01s, \Delta d=0.005, S=1000 W/m^2$

The choice of the value of T_a according to the proposed approach ensures a three-level steady-state duty-cycle swing around the MPP, whatever duty-cycle step-size Δd and irradiance level S are settled, as shown in the plots of the duty-cycle reported in fig. 5, obtained with $T_a=0.01s, \Delta d=0.005$ (fig.5.a), $\Delta d=0.001$ (fig.5.b) and with an irradiance step change from $S=350 W/m^2$ to $S=1000 W/m^2$. Fig. 5.c shows, that a lower value of T_a ($T_a=0.0033s$) leads to a worse behavior of the system characterized, at both irradiance levels $S=350 W/m^2$ and $S=1000 W/m^2$, by a wider swing of the operating point around the MPP. This leads to a lower efficiency with respect to the corresponding case ($T_a=0.01 s$) shown in fig. 5(b). Moreover, in fig. 5(c) at lower irradiance level, a non-repetitive duty-cycle behavior is also evident, in agreement with the experimental results reported in [12].

Whenever a resistive load is considered, the expression of

$$G_{v,d}(s) = \frac{-V_{PV,MPP} \left[2(1-D) \left(1 + s \frac{C_0 R_{MPP}}{2(1-D)^2} \right) \right]}{2(1-D)^2 + \left((1-D)^2 \frac{L}{R_{MPP}} + C_0 R_{MPP} + (1-D)^2 C_i R_{MPP} \right) s + \left((1-D)^2 LC_i + LC_0 \right) s^2 + LC_i C_0 R_{MPP} s^3} \quad (14)$$

the control-to-PV array voltage transfer function $G_{v,d}$, that in the case of the boost battery charger assumes the form (10), becomes as in (14).

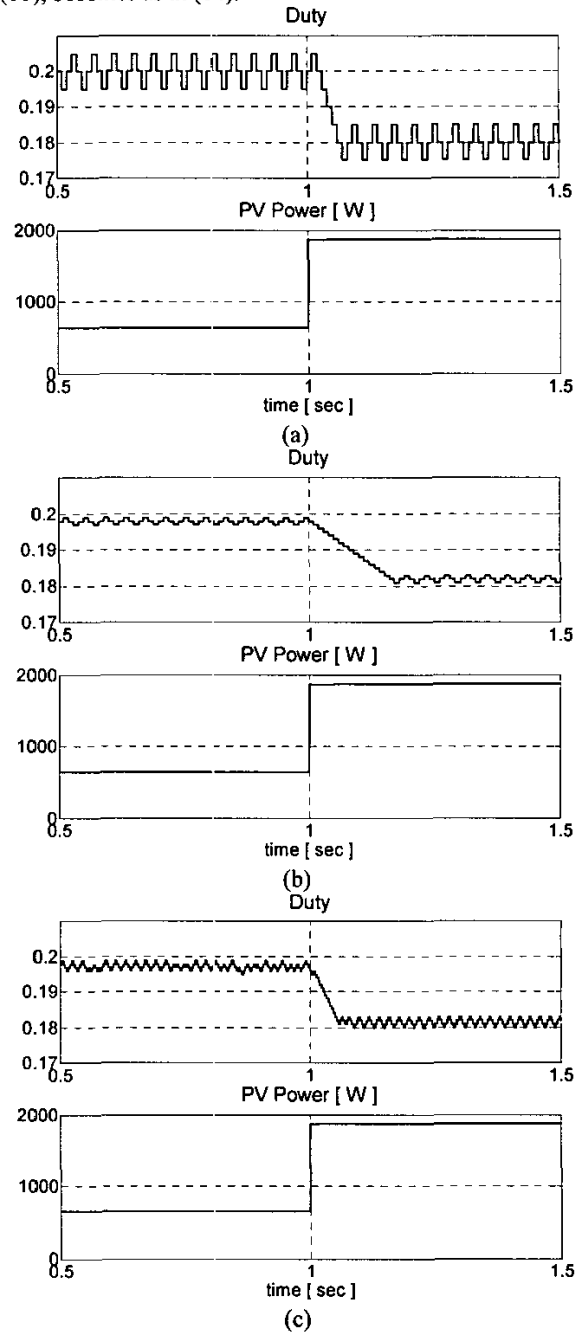


Fig. 5. (a) $\Delta d=0.005, T_a=0.01s$; (b) $\Delta d=0.001, T_a=0.01s$, (c) $\Delta d=0.001, T_a=0.0033 s$

In equation (14), C_o is the output capacitance, D is the quiescent value of the duty cycle at the MPP and $V_{PV,MPP}$ is the photovoltaic array voltage at the maximum power point. In fig.6 the ac model of the system of fig.1 is shown: it has been obtained after the linearization of the photovoltaic array characteristic and of the switching cell.

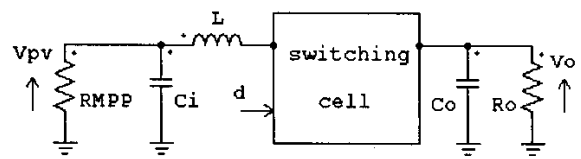


Fig. 6. The ac model used.

It is easy to show that if:

$$C_o \cdot R_{MPP}^2 \gg L \quad (15.1)$$

$$C_o \gg C_i \quad (15.2)$$

then (14) reduces to (10), so that the eqs. (10)-(13) are still valid. When inequalities (15) are not verified or when considering the effect of parasitics that of course render the expression of the transfer function $G_{v,d}$ much more complex, eqs. 10-13 are no more valid. However, what remains valid, is the strategy proposed to optimize the P&O algorithm; such a strategy relies on the choice of T_a according to the dynamic behaviour of the system composed by the dc-dc converter and PV array. Such an approach can be applied to other converters and/or operating modes; whenever the analytical approach is unpractical or unaffordable, it is always possible to get numerically, by means of suitable simulations, the threshold value that T_a must exceed in order to optimize the P&O mppt technique.

IV. CONCLUSIONS

In this paper a theoretical analysis allowing the optimal choice of the value of the sampling period T_a to be adopted when using the P&O mppt algorithm has been carried out. The idea underlying the proposed optimization approach lies in the customization of T_a to the dynamic behaviour of the whole system composed by the specific converter and PV array adopted. As an example, a boost battery charger has been studied in detail.

ACKNOWLEDGEMENTS

This work has been supported by MIUR and University of Salerno grants.

REFERENCES

- [1] S. Liu, R. A. Dougal: "Dynamic multiphysics model for solar array", IEEE Trans. On Energy Conversion, Vol. 17, No. 2, June 2002, pp. 285-294.
- [2] K.H. Hussein, I. Muta, T. Hshino, M. Osakada: "Maximum photovoltaic power tracking: an algorithm for rapidly changing atmospheric conditions", Generation, Transmission and Distribution, IEE Proceedings, Volume: 142 Issue: 1 Jan. 1995, Page(s): 59-64
- [3] M. Veerachary, T. Senjyu, K. Uezato: "Voltage-based maximum power point tracking control of PV system", IEEE Trans. On Aerospace and Electronic Systems, Vol 38, No. 1, January 2002, pp. 262-270.
- [4] K. K. Tse, M. T. Ho, H. S.-H. Chung, S. Y. Hui: "A novel maximum power point tracker for PV panels using switching frequency modulation", IEEE Trans. On Power Electronics, Vol. 17, NO. 6, Nov. 2002, pp. 980-989.
- [5] P. Midya, P. Krein, R. Turnbull, R. Reppa, J. Kimball: "Dynamic maximum power point tracker for photovoltaic applications", pp. 1710-1716.
- [6] E. Koutroulis, K. Kalaitzakis, N. C. Voulgaris: "Development of a microcontroller-based, photovoltaic maximum power point tracking control system", IEEE Trans. On Power Electronics, Vol. 16, NO. 1, Jan. 2001, pp. 46-54.
- [7] T. Noguchi, S. Togashi, R. Nakamoto: "Short-current pulse-based maximum-power-point tracking method for multiple photovoltaic-and-converter module system", IEEE Trans. on Industrial Electronics, Vol: 49, No. 1, Feb. 2002, pp. 217-223.
- [8] K. Irisawa, T. Saito, I. Takano, Y. Sawada: "Maximum power point tracking control of photovoltaic generation system under non-uniform insolation by means of monitoring cells", pp. 1707-1710.
- [9] Chihchiang Hua, Jongrong Lin, Chihming Shen: "Implementation of a DSP-Controlled Photovoltaic System with Peak Power Tracking", IEEE Trans. on Industrial Electronics, VOL. 45, No 1, February 1998.
- [10] Tsai-Fu Wu, Chien-Hsuan Chang, Yu-Kai Chen: "A Fuzzy-Logic-Controlled Single-Stage Converter for PV-Powered Lighting System Applications", IEEE Trans. on Industrial Electronics, VOL. 47, No 2, April 2000.
- [11] I. Batarseh, T. Kasparis, K. Rustom, Weihong Qiu, N. Pongratananukul, Wenkai Wu: "DSP-based Multiple Peak Power Tracking for Expandable Power System", Applied Power Electronics Conference and Exposition, 2003. APEC '03. Eighteenth Annual IEEE, Vol. 1, Feb. 2003.
- [12] D.P. Hohm, M. E. Ropp: "Comparative Study of Maximum Power Point Tracking Algorithms", PROGRESS IN PHOTOVOLTAICS: RESEARCH AND APPLICATIONS, Vol.11, No 1, January 2003.
- [13] N. Femia, G. Petrone, G. Spagnuolo, M. Vitelli: "Optimizing Duty-cycle Perturbation of P&O MPPT Technique", Proceedings of PESC, Aachen (Germany), June 20-25, 2004.
- [14] C. A. Desoer, E. S. Kuh, Basic Circuit Theory, McGraw-Hill, New York, USA, 1969.